



Buss, HL., Mirza, BI., Nash, GR., Storey, C., Buckle, L., Coomber, SD., Emeny, MT., Rarity, JG., & Cryan, MJ. (2008). Measurement of mid-infrared AlInSb light-emitting diodes with surface patterning. In *Conference on Lasers and Electro-Optics and Conference on Quantum Electronics and Laser Science, San Jose* (pp. 1 - 2). Institute of Electrical and Electronics Engineers (IEEE).
<http://hdl.handle.net/1983/1639>

Peer reviewed version

[Link to publication record in Explore Bristol Research](#)
PDF-document

University of Bristol - Explore Bristol Research

General rights

This document is made available in accordance with publisher policies. Please cite only the published version using the reference above. Full terms of use are available:
<http://www.bristol.ac.uk/red/research-policy/pure/user-guides/ebr-terms/>

Measurement of Mid-infrared AlInSb Light-Emitting Diodes with Surface Patterning

I.J. Buss*, B. I. Mirza*, G.R. Nash*†, C. Storey†, L. Buckle†, S. D. Coomber†, M. T. Emeny†, J.G. Rarity* and M.J. Cryan*

*Photonics Research Group, Department of Electronic and Electrical Engineering,
University of Bristol, Bristol, BS8 1UB, UK, Email: ian.buss@bristol.ac.uk
†QinetiQ, Malvern Technology Centre, Malvern, WR14 3PS, UK

Abstract: 3D FDTD modelling is employed to design a surface pattern for mid-IR LEDs. Measured enhancement factors over an un-patterned device of 8% and 14% are found at 300K and 25K respectively.

© 2008 Optical Society of America

OCIS Codes: (230.3670) Light-emitting diodes; (240.5770) Roughness

1. Introduction

Mid-infrared light-emitting diodes (LEDs) are the subject of much research and have great potential in such applications as gas sensing (in the wavelength range $\lambda = 3 - 10\mu\text{m}$) and free-space quantum communications [1,2]. Some of the high brightness LEDs at these wavelengths that have been recently reported [3], were fabricated from $\text{Al}_x\text{In}_{1-x}\text{Sb}$, where the peak emission wavelength can be tailored by varying the aluminium content. However, the extraction efficiency from such devices is limited in great part by the phenomena of total internal reflection and Fresnel reflection from the dielectric boundary at the surface of the devices. In general a factor of $1/n(n+1)^2$ of the light generated within a device is prevented from escaping from the device by these effects [4]; in AlInSb this implies that a mere 1% of the generated light will escape in an un-optimised device. A method that has been applied at visible wavelengths is to pattern the surface of the device to either promote extra emission via grating effects or through the randomisation of internal photon trajectories when coupled with a recycling mirror [5,6]. This paper presents data from mid-IR devices that have been patterned with a disordered periodic grating via E-beam lithography. The structure of the devices is described in detail in references [3,7]. The etched pattern is designed using a 3D Finite-Difference Time-Domain (FDTD) modelling method which assesses the enhancement it provides.

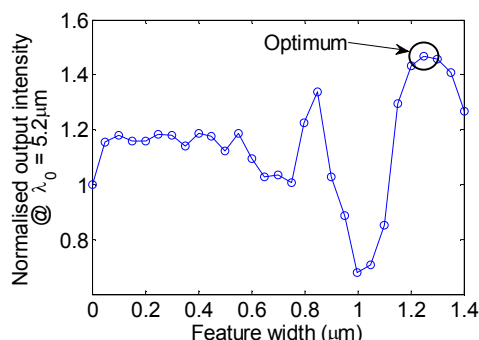


Fig. 1: Output intensity for different pattern widths normalised to an un-patterned surface at $\lambda_0 = 5.2\mu\text{m}$.

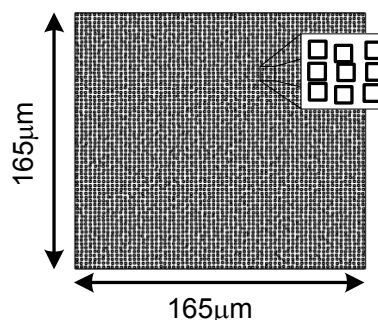


Fig. 2: Pattern etched on to the surface of the device pixels and inset showing zoom-in.

2. FDTD Modelling

The surface patterns are investigated using an in-house 3D FDTD code which has been used extensively in the design and modelling of optical devices, in particular photonic crystal based structures [3]. The model consists of a simulation space $10 \times 5 \times 10\mu\text{m}$ in size, with the lower part of the space is occupied by a block $10 \times 3.5 \times 10\mu\text{m}$, while the remaining $1.5\mu\text{m}$ is free space. The block has an index of refraction $n_s = 3.96$ representing an AlInSb LED in the mid-infrared. A single dipole excitation polarised in E_x is placed in the lateral centre of the block $1.5\mu\text{m}$ from its surface in order to represent an emitter in the active region. It is excited with a broadband Gaussian modulated sinusoid pulse, centred at $\lambda_0 = 5.2\mu\text{m}$. The space is meshed with 8 million cells and run for 10,000 time steps. The emission from the dielectric is monitored at 81 probes placed $0.5\mu\text{m}$ above the surface of the block which record the time-evolution of the electromagnetic field. The data from these probes is Fourier transformed and summed to give the emission intensity at a specific wavelength. The model is illustrated in Figure 2, with an applied surface pattern.

Various parameters of the surface pattern are investigated including the width w and depth d of the surface features and mark-space ratio m and degree of disorder s expressed as a standard deviation. It is determined that the

optimum pattern is one with feature widths of $w = 1250\text{nm}$ when $d = 400\text{nm}$, $m = 0.5$ and $s = 0.2\mu\text{m}$, as shown in Figure 1. This pattern shows an approximate enhancement of 1.47 over an un-patterned surface. These data are used to design a surface pattern to be etched on to the surface of the device pixels and is illustrated in Figure 2.

3. Experimental Measurements

The optimum modelled pattern was transferred to each element [7] of three LED devices using e-beam lithography and wet chemical etching. The etch times (24, 36 and 48 seconds) were varied to vary the depth of the pattern. Measurements are underway to determine the exact depths these etching times provide. The patterned devices were compared to an un-patterned device. Initially, I-V characteristics were measured to confirm that the etching process had not degraded the electrical performance of the devices. Total integrated powers and calibrated spectra were then measured at both room temperature (300K) and at low temperature (25K), with the devices mounted on the cold-finger of a closed-cycle cryostat. Emitted Light was collimated by a lens and directed either directly to a pre-calibrated 77K HgCdTe photo-detector, mounted on an x-y stage, or to a SPEX 270M grating spectrometer and then on to the photo-detector. Correction factors were applied to account for the losses due to the optics.

The total integrated powers for each device were measured by scanning the detector over an area $4 \times 4\text{mm}^2$ and are given in Table 1. In two of the patterned devices a significant increased total integrated power is seen, with a 14.4% increase for device 2 at $T = 25\text{K}$ and an 8.8% increase for device 4 at $T = 300\text{K}$ compared with the un-patterned device. Larger numbers of devices will now be assessed in order to fully understand the trends in these results.

The total integrated powers were then used to calibrate the spectra measured using the spectrometer, and results from the two devices showing the greatest emission are plotted together with the data from an un-patterned device in Figure 3. The large dip in the response at $\lambda_0 = 4.25\mu\text{m}$ is due to carbon dioxide absorption. The peak emission from these devices is at $\lambda_0 = 4.5\mu\text{m}$ at $T = 300\text{K}$ and at $\lambda_0 = 4.0\mu\text{m}$ at $T = 25\text{K}$. This is slightly removed from the design wavelength and could account for some of the reduction in enhancement.

Table 1: Total integrated powers at 25K and 300K

Device	Power @ 25K ($\mu\text{W}/\text{cm}^2$)	Power @ 300K ($\mu\text{W}/\text{cm}^2$)
1 (Flat)	29.0	37.4
2 (24 s)	33.2	38.4
3 (36 s)	30.2	32.0
4 (48 s)	30.1	40.7

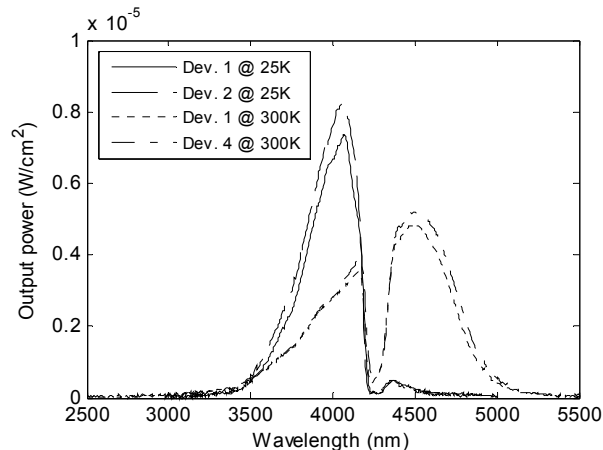


Fig. 3: Room temperature (300K) calibrated spectra for a patterned and un-patterned device.

4. Conclusion

This paper presents initial modelling and experimental measurements of mid-infrared AlInSb LEDs. A surface pattern intended to improve light extraction from the devices was designed using 3D FDTD modelling which investigates the pattern width, depth and disorder. This pattern was etched onto the surface of three devices for differing etching times. These devices were measured and compared with an un-patterned device at $T = 300\text{K}$ and $T = 25\text{K}$. Output enhancements of 8.8% and 14% were seen for two patterned devices.

5. References

- [1] S. D. Smith *et al.*, "Comparison of IR LED gas sensors with thermal source products," IEE Proc.: Optoelectron. **144**(5), 266-270 (1997).
- [2] G.R. Nash, *et al.*, "Lateral n-i-p junctions formed in an InSb quantum well by bevel etching," Semicond. Sci Tech. **20**, 144-148 (2005).
- [3] M.K. Haigh, *et al.*, "Mid-infrared $\text{Al}_x\text{In}_{1-x}\text{Sb}$ light-emitting diodes," Appl. Phys. Lett. **90**, 231116 (2007).
- [4] T.S. Moss, G.J. Burrell and B. Ellis, Semiconductor Opto-Electronics, (Butterworths, London, 1973), Chap. 1.
- [5] W.K. Wang, *et al.*, "Fabrication and efficiency improvement of micropillar InGaN/Cu light-emitting diodes with vertical electrodes," Appl. Phys. Lett. **88**, 181113 (2006).
- [6] B.A. Matveev, *et al.*, "3.3 μm high brightness LEDs," in Mater. Res. Soc. Symp. Proc. Vol. **891**. (Materials Research Society, 2006), pp. 9-14.
- [7] H. R. Hardaway, T. Ashley, L. Buckle, M. T. Emeny, G. Masterton, and G. Pryce, Proc. SPIE 5564, 105 (2004).
- [8] I.J. Buss, *et al.*, "3D Modelling of Enhanced Surface Emission using Surface Roughening," CLEO US, May 2006.